Journal of Hydraulic Structures
J. Hydraul. Struct., 2022; 8(1): 67-81
DOI: 10.22055/JHS.2022.40476.1211

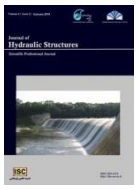

OPEN ACCESS

Numerical Simulation of the effect of L-shaped spur dike wing length on scouring at a 90 ° bend

Mousa Rasaei[1]

Abstract

Spur dike is one of the common structures in organizing and controlling erosion on the river bank. On the other hand, the placement of the spur dike in the bended part of the river, while removing strong currents from the shore and directing the flow to the river axis, also changes the flow pattern and scour around the spur dike. The aim of this study was to numerically investigate the effect of length change in L-shaped Spur dike wing on scour depth located in a channel with a 90° bend. For this purpose, the three-dimensional SSIIM numerical model was used for simulation. L-shaped spur dikes with different wing lengths were tested and simulated. At the end, the outputs of the numerical model were compared with the laboratory results and validated. The results while confirming the SSIIM numerical model in scour simulation around the spur dike showed that by increasing the length of the spur dike wing and decreasing the angle of the spur dike in the bend, the depth and volume of the scour decreases significantly. In addition, the maximum depth and volume of scour around the spur dike was recorded at a 90 ° angle with a length to web ratio of 0.5. On the other hand, in all cases, scour around the simple spur dike was more than the L-shaped spur dike with different wing lengths.

Keywords: L-shaped Spur-dike, wing length change, scouring, SSIIM and numerical model.

Received: 08 April 2022; Accepted: 04 June 2022

1. Introduction

Destruction and erosion of river banks, especially in bends, is a natural and undeniable thing that causes a change in the morphology of rivers as well as a change in the ownership of coastal lands for individuals. Therefore, it is necessary to deal with this. The phenomenon should be considered and somehow stabilized and protected the river banks. One of the possible measures is the construction of a spur dike. Spur dikes are structures that are constructed with the aim of diverting the flow from the erodible shore of the river or creating a suitable path to direct the flow and control the flood and in fact establish the necessary depth for shipping purposes [1]. Although the spur dike is constructed with the aim of depositing and preventing erosion of the river banks and margins and stabilizing the position of the river, at the same time they are affected by the

[1] Department of Civil Engineering, Islamshahr Branch, Islamic Azad University, Islamshahr, Iran. rasaei.iau@gmail.com

phenomenon of erosion. In general, the erosion is mainly due to the concentration of flow, especially in the nose, local increase in flow velocity due to cross-sectional constriction and the occurrence of downward rotational flow. Due to the erosion phenomenon, scour hole is formed around the spur dike in such a way that its development endangers the strength of the structure. Of course, this is exacerbated in bends due to the presence of strong rotational flows. Therefore, it is necessary to take measures to protect the spur dike (Fig 1). Achieving this requires knowing the amount of depth and volume of scour around these structures [2]. It should be noted that there are different types of spur dikes and one of the most common and widely used is L-spur dike.

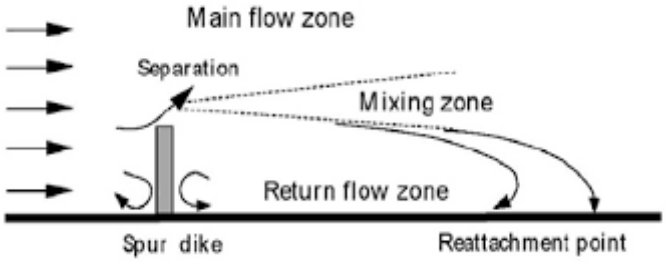

Figure 1. Flow around the spur dike [3]

The scour around spur dikes has long been considered by various researchers. This researches by considering different hydraulic conditions in laboratory [4-8] and numerically [9-12] has been done. In recent years, with the provision of favorable laboratory conditions and access to advanced and modern numerical simulation systems, more comprehensive research has been done. The following are some of the most important researches done. In 2011, Ghobadian and Mohammadi [13] used the SSIIM numerical model to simulate in-stream flows. Vaghefi et al. [14] examined the effect of spur dike length, wing length of spur dike, spur dike location on the bend, bend radius and current intensity around the T-shaped spur dike in a bended channel. They were able to provide an equation for determining the amount of scour around the T-shaped spur dike. Karami et al. [15] using experimental data, they confirmed that the SSIIM numerical model based on the finite volume method has the ability to simulate the scouring phenomenon around the spur dike. In 2017, Kiani et al. [16] introduced an experimental relationship with a high regression coefficient of 96% to determine the maximum scouring depth around the spur dike series based on laboratory observations. Vaghefi et al. [17] examined the scour around the T-shaped spur dike at a 90 ° bend. They found that the secondary flows started at an angle of 30 degrees and continued decreasingly to an angle of 65 degrees. Olsen et al. [18] developed the SSIIM numerical model for modeling sediment transport. Ning et al. [19] investigated the effect of distance between spur dike on scour and flow pattern using a numerical model. Omenzadeh et al. [20] the effect of spur dike length on scour depth was investigated at 90 and 180 ° bends. In this study, they used a channel with a 180 ° bend with an R/B ratio of 4.7. The results of this study showed that with increasing the length of the spur dike, the depth of scouring also increases significantly. In addition, increasing the flow rate and the location of the spur dike in the bend leads to an increase in the dimensions of the scour hole and sediment ridge. In 2020, Yarahmadi et al. [21] investigated local scouring around a new type of triangular-nose culvert. They used different hydraulic conditions in this study. In addition, the results were compared with a rectangular culvert and analyzed. In general, their results of 44% and 70% reduction, respectively, gave the maximum depth and volume of scour around the trunk

with a triangular nose compared to the ruler with a rectangular nose. Rasaei et al. [22-24] studied the scour around the bridge piers in a channel with a 90° convergent bend using the SSIIM numerical model. In 2021, Tripathi and Pandey [25] used a laboratory model to investigate the scouring status around the T-spur dike located in a 180° bend channel. Their results showed that local scouring around the spur dike increases with increasing landing number and location in the bend.

A review of studies so far shows that researches have mainly evaluated the scouring situation around the spur dikes in terms of the effect of changing the hydraulic parameters in straight and sometimes bended channels and the effect of geometric parameters has not been less considered. Therefore, in this study, the effect of changing the spur dike length as a very effective geometric parameter in reducing the amount of scour around L-shaped spur dikes in 90° bend channels has been evaluated numerically. The SSIIM numerical model based on finite volume method was used and changes in maximum depth and volume of scour cavities were investigated and compared with laboratory results and validated.

2. Material and Methods

2.1. SSIIM numerical model

The numerical model used in this research is known as the SSIIM numerical model. An introductory version of this model was developed by Olsen in 1991 at the Norwegian Institute of Technology and has been developed in recent years [26]. In general, the use of SSIIM model in river engineering applications, environmental engineering, and hydraulics Sediment transfer is continued and with its development, the use of this model was extended to other hydraulic applications. The SSIIM numerical model is based on the finite volume method and solves the Navier-Stokes equations typically using with the standard *K-ε* turbulence model in an almost orthogonal three-dimensional grid. The main advantage of the SSIIM model over other computational fluid dynamics programs is its ability to model sediment in the living bed and in complex geometries. Also this model of volume control method with the power rule algorithm, or the second-order algorithm, uses the method for breaking the equations, and the method for the pressure and velocity coupling. In this model, the velocity field is calculated by an implicit solution method and solved by solving the sediment continuity equation. The Navier-Stokes equation for a non-compressible, constant-density current is expressed as follows.

$$\frac{\partial U_i}{\partial t} + U_j \frac{\partial U_i}{\partial Xi} = \frac{1}{\rho} \frac{\partial}{\partial X_i} (P\delta_{ij} - \rho \overline{u_i u_j}) \quad (1)$$

In the above equation, the first sentence on the left, the transitive and time-dependent expression, the next sentence, the transferable expression, the first sentence on the side right, the parameter is related to pressure and the last sentence is the parameter related to Reynolds's stress.

In SSIIM numerical model, sediments are divided into two parts by suspension and by surface so that for calculation by suspension from equation distribution transfer is used as follows:

$$\frac{\partial_C}{\partial t} + U_j \frac{\partial C}{\partial X_j} + \omega \frac{\partial C}{\partial Z} = \frac{\partial C}{\partial X_j} (\Gamma_\Gamma \quad \frac{\partial C}{\partial X_j}) \quad (2)$$

Where, C is sediment concentration, ω is fall velocity, U is flow velocity, x is distance, Γ_Γ is diffusion coefficient.

2.2. Numerical simulation process

2.2.1. Models and laboratory data used in numerical simulation

Since, the purpose of this research is to simulate scouring around L-spur dike with different wing lengths. Therefore, the model, data and laboratory results of Divsalar and Musavi-Jahromie [3] were used in the simulation process and validation of the numerical model according to the plan of figure 1. The model in question is a Plexiglas channel with a 90° bend and a central radius of 3.15 meters. Two straight channels with lengths of 6.00 and 3.00 meters are formed upstream and downstream of the bend, respectively. One the other hand, the width and height of the channel are fixed along the entire length of the channel and are 70 and 60 cm, respectively (Fig 2a). Also, in this study, a simple spur dike and an L-shaped spur dike with different wing lengths according to Figure (2b) were used. Table 1 shows the range of parameters affecting the scour around the L-shaped spur dike.

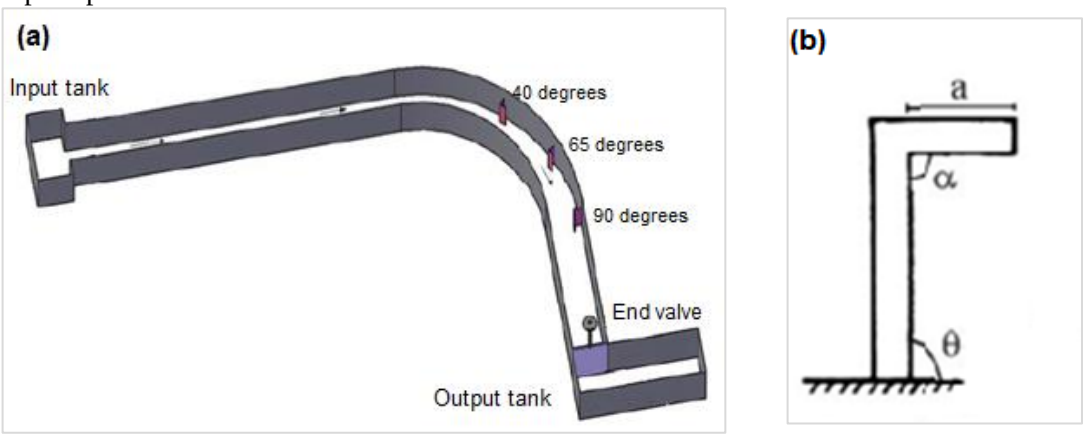

Figure 2. Laboratory model: a) Flume, b) L-shaped spur dike with different lengths

Table 1. Range of effective parameters

effective parameters	Range of changes
Flow discharge	29.2 l/s
Upstream depth	15.3 cm
The length of the spur dike web	14 cm
The length of the spur dike wing	7, 10.5, and 14 cm- simple spur dike
Froude number	0.22
Spur dike position	40, 65, and 90 degrees

2.2.2. Geometry model networking

As mentioned earlier, the channel considered in the simulation process is exactly the same as the laboratory flume used in laboratory studies of Divsalar and Musavi-Jahromie [3]. By running the SSIIM numeric model, a set of input files is included KOORDINA FILE includes field network coordinates and CONTROL FILE contains program control information. In these files, the necessary information is entered according to the software structure. The first step before starting the simulation process is to discretize the field amplitude into the cells that govern the differential equations. For this purpose, different meshes with different sizes and based on the results of analysis and mesh sensitivity analysis was tested for simulation at 90 ° bends. Since, the channel is bended, the structured networks cannot be used in modeling. Therefore, to draw the bended part of the channel, its coordinates in excel software defined and stored in KOORDINA

file according to SSIIM software. In the direct downstream and upstream parts of the channel, structured networks (regular blocks) were used in the software. In general, in order to increase the accuracy of field geometry calculations, it was tried to define the mesh size near the spur dike and the boundary between the bended section of the channel and the upstream and downstream channels is considered the finer meshes. Therefore, in the bended section of the channel, one network line was considered for each degree. In general, in the bended section of the channel and in the direction of axis I, 91 network lines and in the direction of axis j, 36 lines with X /Y ratio = 2.6 were considered. In the direct upstream and downstream sections of the channel, in order to reduce the computation time, larger meshes with X /Y= 2 ratio were also used. Furthermore, in all cases, meshes with ratio *X/Y* = 3.61 were used in the vertical direction of the channel. Table 2 and Figure 3 show the meshing analysis results of the bend, upstream, and downstream channels.

Finally, after the channel drawing and networking, channel geometry coordinates were recorded in KOORDINA file. In total in this study, about 6 types of meshes with different sizes and configurations were tested and finally 19026 cells as the optimal number of cells in the analysis and numerical analysis was used. Although reducing the mesh size increased program execution time, more accurate results were obtained. Figure 4 shows a schematic view of the networking used in this research.

Table 2. Results of mesh sensitivity analysis

The number of cells considered in the bend section	The number of cells considered in the direct channel upstream	The number of cells considered in the direct downstream channel	The number of cells considered in the direct downstream channel	ds/dy (Numerical)	s/dy (Experimental)	percentage error
1638	5250	2625	9513	Divergence	1.06	100.00
2093	7000	3500	12593	0.99	1.06	7.07
3276	10500	5250	19026	1.08	1.06	1.85
4777	14000	7000	25777	1.175	1.06	9.79
6370	21000	10500	37870	Divergence	1.06	100.00

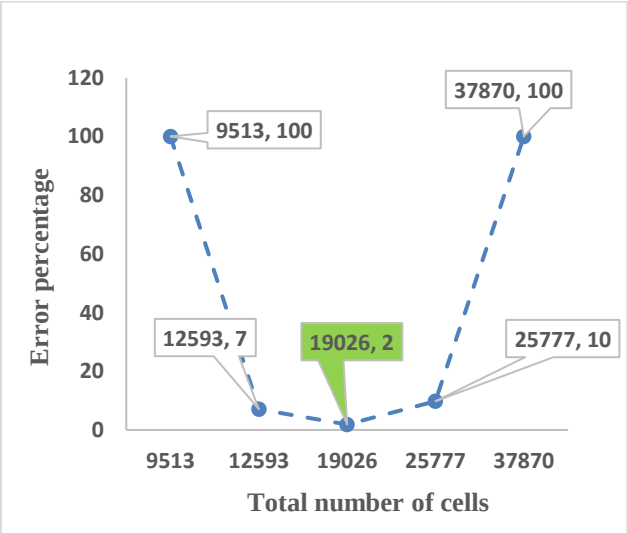

Figure 3. Sensitivity analysis chart and number of optimal meshes

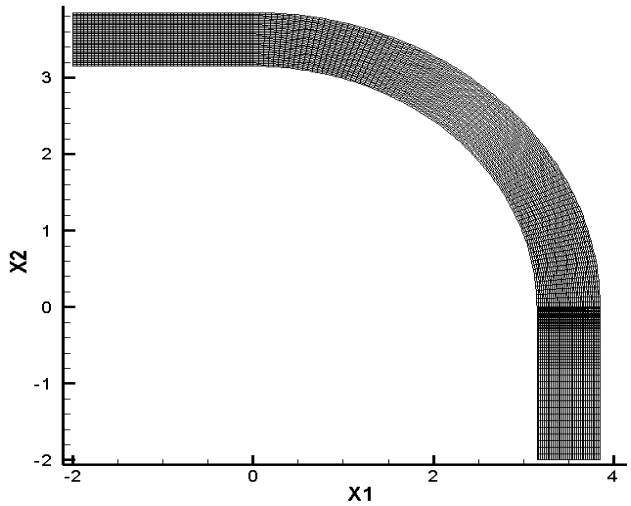

Figure 4. Channel mesh network

Other parameters such as hydraulic flow and sediment conditions, boundary conditions, roughness coefficient, methods for solving the governing equation, time steps, etc. were also introduced in the CONTROL FILE. Next, the simulation process by calling the KOORDINA and CONTROL files and the simulation and computation process begins. When the calculations are completed, the results Simulations such as velocity components, shear stresses, water level and maximum scour depth in a file called RESULT Turns. In this step, TECPLOT software was used to draw and display different lines. For model calibration SSIIM, a wide range of the above parameters was assigned to the software and after several executions, the most compatible Parameters were selected between numerical and experimental models and used in other simulations.

2.2.3. Validation and calibration of SSIIM numerical model

Before using the numerical model in simulating the flow and scour pattern around the L-shaped spur dike, it is necessary to calibrate and the accuracy of the numerical model was ensured. For this purpose, first a numerical simulation test, with the aim of determining the equilibrium time in experiments and the maximum depth of scour around the spur dike was calculated at 29.2 L/S at 90 degrees. Border conditions and various turbulence models in simulation were investigated and evaluated. According to the diagram of Figure 5 extracted from Numerical simulation shows that 87% of scouring occurred in the first 125 minutes. On the other hand, it is observed that the equilibrium time diagram in the numerical model is in good agreement with the experimental model diagram, which shows the confirmation of the simulation and calibration has a numerical model. Finally, the most optimal parameters extracted from the model calibration according to table 3 are extracted and was used in later simulations.

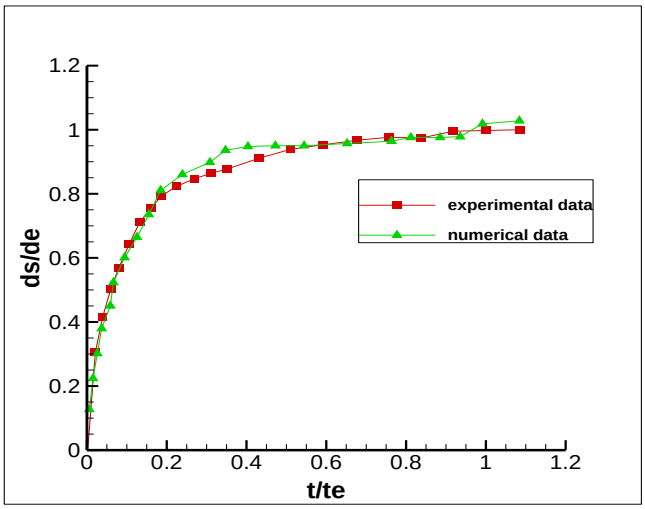

Figure 5. Equilibrium time diagram in laboratory and numerical model

Table 3. Parameters extracted from calibration of numerical model

Boundary conditions	Time step	Number of internal repetitions	Transient sediment calculation algorithm	The method of discretizing the governing equations	Bed particle transfer method	The turbulence model
k-ε	10	10	TSC	POW	Van rain	Wall law

3. Results and discussion

Since, the purpose of this study is to numerically investigate the effect of changing the length of the L-shaped spur dike wing on the scour around the spur dike located at a channel with a 90° bend. For this purpose, by modeling a spur dike with different wing length and placement at different angles from the 90° bend, the position of the flow pattern and guttering around the spur dikes, taking into account the most important parameters affecting the following was reviewed and evaluated.

3.1. Effect of spur-dike position on local scour

Placement of the spur dike at different angles of a 90 ° bend channel in addition to changing the flow pattern on the bed topography and the maximum scour depth around the spur dike had a significant effect. Figure 6 an example of the effect of the spur dike position with wing length of 7 cm on bed level changes and scouring, under the effect of 29.2 liters per second and at 40, 65 and 90 degrees. In this figure, the 1x and 2x axes are the number of divisions in the horizontal and vertical directions of the graph, respectively. As can be seen, the depth and volume of the scour are increased by changing the position of the spur dike to the downstream of the bend. This can be attributed to the effect of centrifugal force on the flow, which causes the formation of a strong transverse flow in the bend. As a result of combining the transverse flow with the longitudinal flow of the path, the famous helical flow emerges. This flow takes on a more complete shape as it progresses downward and to the end of the bend. Then, as the helical flow passes through the bend, this flow exits the channel in an extended manner. On the other hand, the placement of the spur dike in the flow path and the collision of the flow with the spur dike increases the intensity of this process. According to Figure 6(a), it can be seen that at an angle of 40 degrees, major

scouring has occurred in two oval areas, both of which have been created in front of the spur dike wing in the center of the bend. It is observed that scouring starts from the middle of the spur dike and extends inclined towards the center of the bend so that the maximum depth and volume of scouring occurred in front of the spur dike wing and its downstream in the center of the bend. On the other hand, with the passage of flows and sediments arising from the scour hole due to eddy flows created in the downstream of the spur dike, we see the deposition and deposition of a significant amount of sediments in a wide radius inclined to the inner wall of the bend. The software outputs show the maximum depth and volume of scouring at an angle of 40 degrees, 14.08 cm and 89270 cm3, respectively (Fig 6a). With increasing position of the spur dike in the bend and entering the angle of 65 degrees, it is observed that the intensity of shear stresses and eddy flows around the spur dike has increased. The results show that the maximum depth and volume of scour are 14.9 cm and 91023 cm3, respectively (Fig 6b). Then, reaching the end of the bend and at an angle of 90 degrees, it is observed that the maximum amount of scouring is oval in front of the spur dike wing in the center of the bend perpendicular to the flow axis. In this area, scouring begins at the center of the bend-sloping channel with a value of 15 cm, and as it leans toward the walls, it decreases and decreases to almost zero. The results show that the maximum depth and volume of scour are 15.3 cm and 98847 cm3, respectively (Fig 6c). The results of other numerical simulation tests show that in all cases, the depth and volume of scour increase with increasing position of the spur dike in the bend. In the second half of the bend and at an angle of 90 degrees, the depth and volume of scour around the spur dike reaches its maximum.

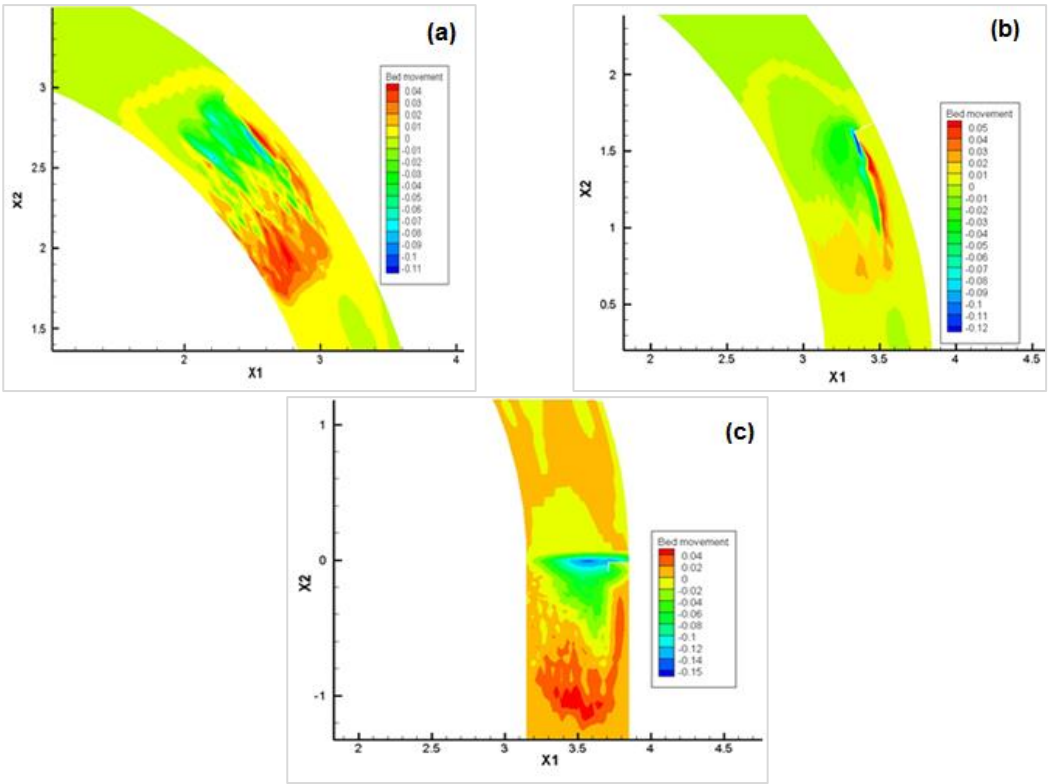

Figure 6. Bed topography and maximum scour depth around the L-shaped spur dike with a wing length of 7 cm, a) 40 ° angle, b) 60 ° angle, c) 90 ° angle

Figure 7 shows the numerical and laboratory comparison of changes in the maximum scour depth around the L-shaped spur dike at different angles. As can be seen, the numerical simulation results are in good agreement with the laboratory results. On the other hand, in all cases, with increasing the position of the spur dike in the bend, the maximum scouring depth also increases.

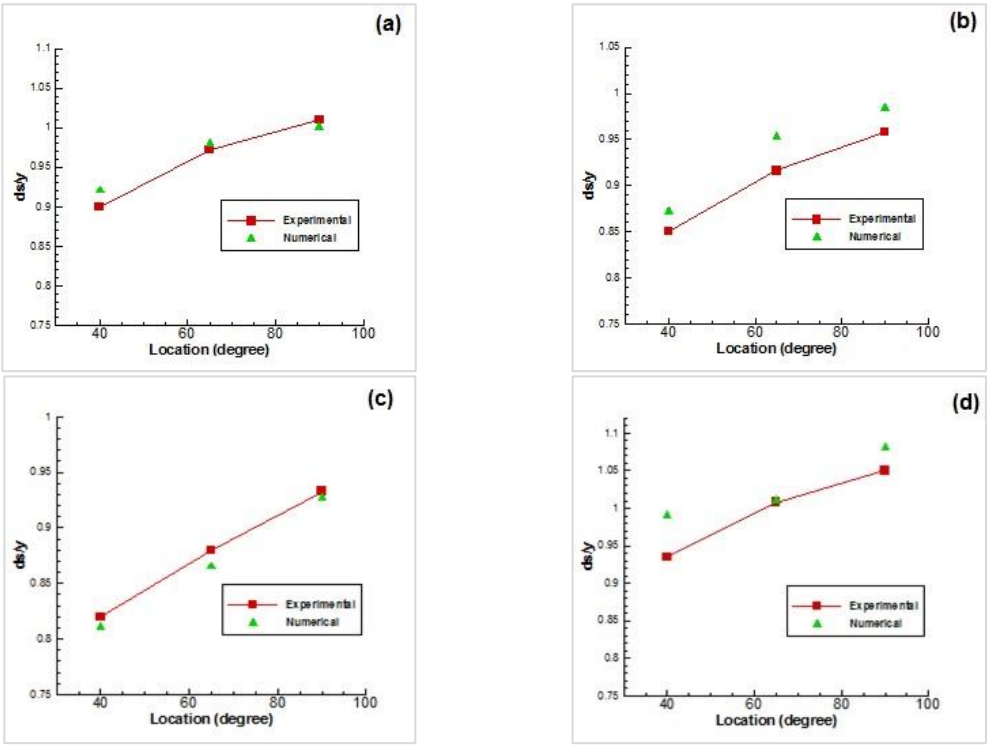

Figure 7. Comparison of changes in the maximum scour depth around the simple and L-shaped spur dikes with different wing lengths located in different positions of the 90 ° bend, a) spur dike with wing length 7 cm, b) spur dike with wing length 10.5 cm, c) spur dike with wing length 14 cm, d) Simple spur dike

3.2. Effect of spur-dike wing length change on horizontal velocities within the channel and around the spur-dike

Figure 8 shows the velocity and intensity vectors around the L-shaped spur dike with different wing lengths at an angle of 90 °. As can be seen in all cases the flow velocity at the boundary of the direct upstream channel and the upstream input of the bend is increased. As the flow enters the bend, especially in the first half of the bend, due to the dominance of the centrifugal force over the lateral pressure gradient, the flow lines are inclined towards the outer wall of the bend. The flow velocity increases dramatically to a 45° angle at the apex of the bend. On the other hand, it is observed that in this area the flow velocity at the inner edges of the bend is at its minimum. With the entry of the flow into the second half of the bend and at an angle of 90 degrees and the collision of the flow with the spur dike wing, the density of flow lines and consequently the flow velocity in the spur dike wing range decreases and reaches its minimum value. As the flow passes through the spur dike body, it is observed that the flow velocity begins to increase and the flow lines are inclined towards the inner wall of the channel. According to the images in Figure 8, it is clear that the maximum horizontal velocity started from the tip of the spur dike wing and occurred up to the

middle of the direct outlet channel. It is important to note that the flow velocity behind the spur dike is reduced, which can be due to the lack of flow penetration and thus reduce the intensity of eddy flows in this area.

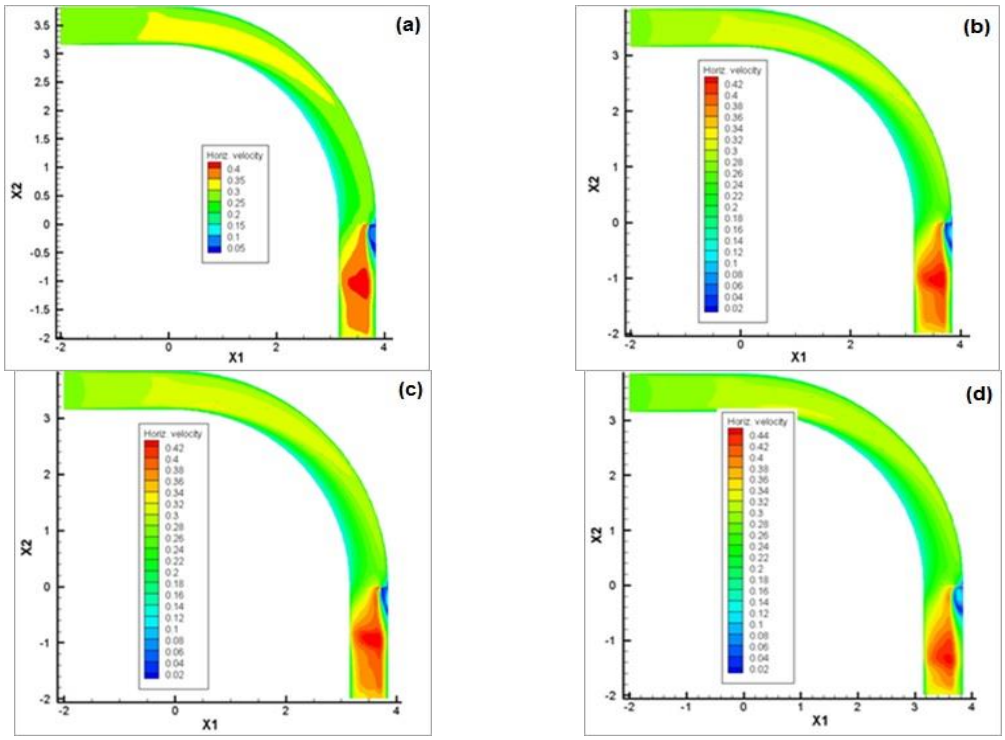

Figure 8. Horizontal velocity contours around a simple spur dike and an L-shaped spur dike with different wing lengths, a) spur dike with wing length 7 cm, b) spur dike with wing length 10.5 cm, c) spur dike with wing length 14 cm, d) Simple spur dike

Figure 9 shows a comparison of changes in the maximum horizontal velocity around an L-shaped spur dike with different wing lengths and a simple spur dike located at a 90° angle. It is observed that with increasing the length of the spur dike wing, the intensity of the flow velocity around the spur dike is reduced. On the other hand, it is clear that in all cases, the velocity of the flow around the simple spur dike is higher than the L-shaped spur dike with different wing lengths

.

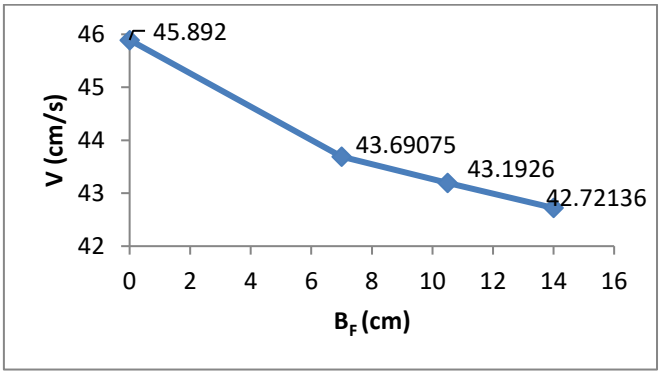

Figure 9. The maximum horizontal velocity changes around a simple spur dike and an L-shaped spur dike with different wing lengths located at a 90° angle.

3.3. The effect of changing the wing length to the web of spur-dike on scouring

Figure 10 shows the position of the scour hole around simple and L-shaped spur dike with different wing lengths at a critical position of 90 °. As can be seen in figures 10 (a, b and c), with increasing the length of the spur dike wing, the shear stresses and as a result, the dimensions and volume of the scouring hole around the spur dike have decreased significantly. The outputs of the numerical model show that increasing the length of the spur dike in dealing with longitudinal flows leads to further failure of the flow and consequently the wear and tear of the vortex and secondary flows over a large area around the spur dike. It should be noted that in this mode, the maximum depth and volume of scouring has also decreased. Figure 10d shows the condition of the scour hole around a simple spur dike. It is observed that the dimensions of the scour hole around the simple spur dike are larger than the L-shaped spur dike with different wing lengths. Because a simple spur dike has a lower contact surface with the flow, the velocity and intensity of the flow will naturally increase, and vortex flows will form more fully around and behind the spur dike. As a result, the size, depth and volume of the scouring hole also increase. The output graphs of the numerical model show that by increasing the length of the L-shaped spur dike wing and the distance of the vortex flows, in turn, had a significant effect on the transfer of materials downstream of the spur dike.

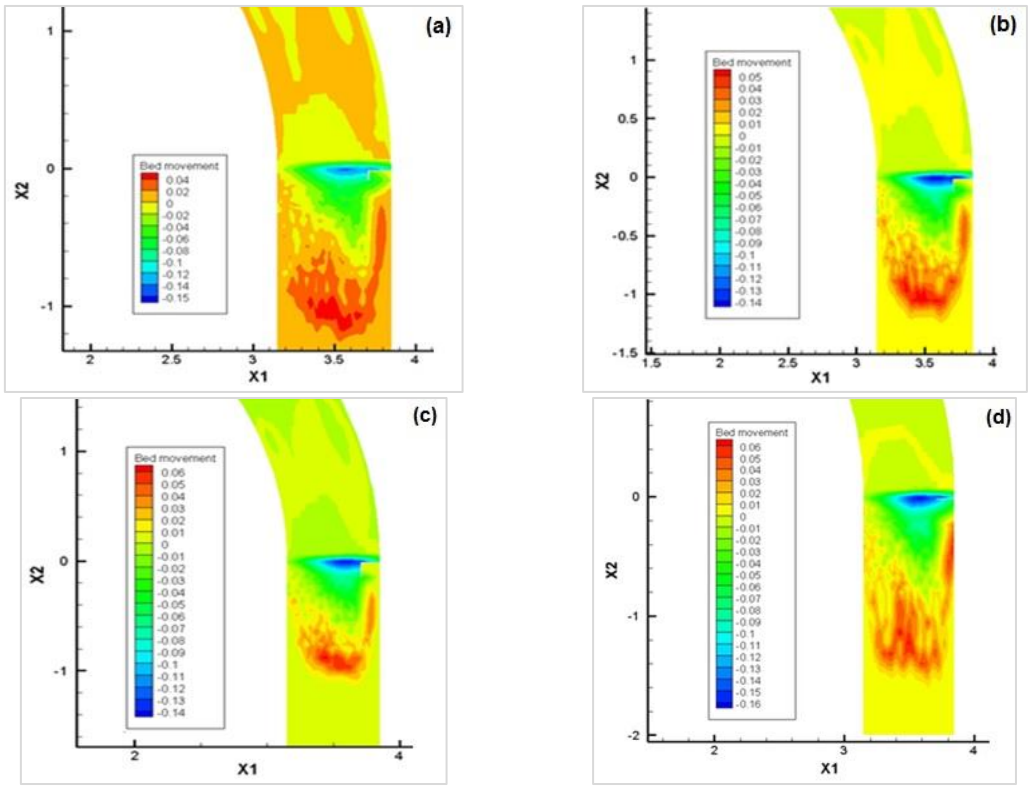

Figure 10. The scouring hole around the spur dike with different wing lengths, a) spur dike with wing length 7 cm, b) spur dike with wing length 10.5 cm, c) spur dike with wing length 14 cm, d) Simple spur dike

On the other hand, a comparison of the effect of length change to spur dike web (B/W) on the maximum scour depth in different situations in both numerical and laboratory models can be seen

in the diagrams in figure 11. It is observed that in all cases, the maximum depth of scouring decreases with increasing wing-to-web ratio. The results and outputs of the numerical simulation, while confirming the SSIIM numerical model in scour simulation, show that the lowest scour depth occurred in the spur dike with a wing-to-web ratio of 1.

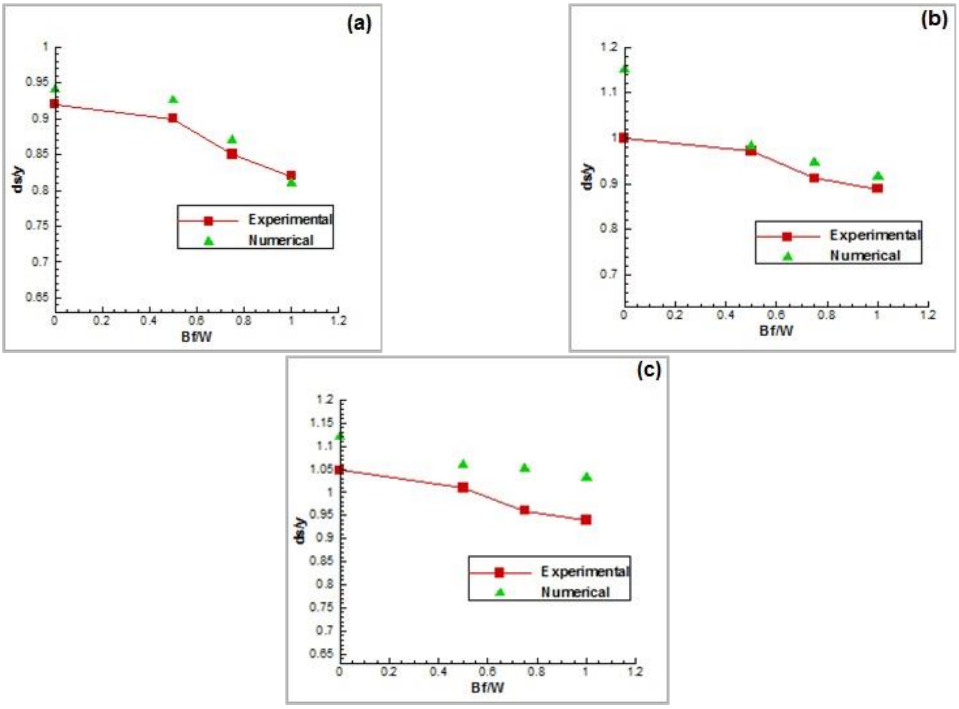

Figure 11. Numerical and laboratory comparison of changes in the maximum scour depth around the spur dike with different wing lengths and in different positions, a) 40 ° angle, b) 60 ° angle, c) 90 ° angle

Figure 12 shows the volume changes of the scour around the simple spur dike and the L-shape with different wing lengths at an angle of 90 degrees. It is observed that in all cases, the amount of scour decreases with increasing the length of the spur dike wing. On the other hand, the volume of scour around the simple spur dike is much larger than the L-shaped spur dike with different wing lengths.

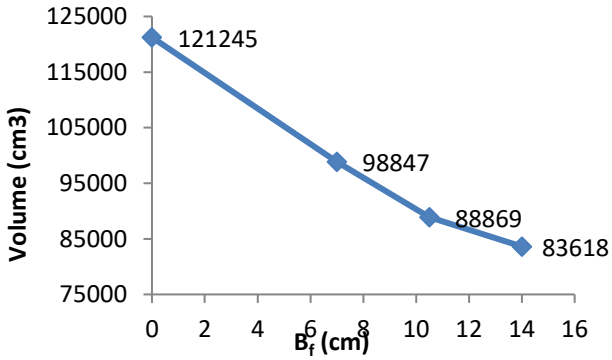

Figure 12. Scour volume changes around a simple, L-shaped spur dike with different wing lengths at a 90° angle

Figure 13 shows the laboratory and numerical comparison of the maximum scour depth values around the L-shaped spur dike with different wing lengths and a simple spur dike. As can be seen, the results have a good correlation of $R^2 = 0.91$.

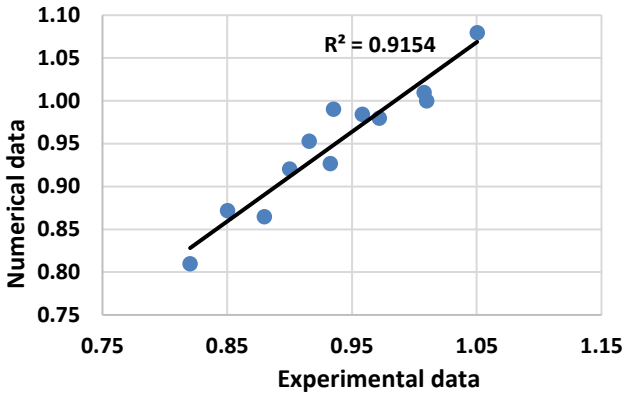

Figure 13. Comparison of maximum scour depth values obtained from laboratory work and numerical results

4. Conclusions

Since the purpose of this study is to investigate the effect of changing the length of the l-shaped spur dike wing on the amount of local scouring located in a 90° bend, the research results are summarized as follows.

In all testes, the maximum depth and volume of scour around the simple spur dike was observed more than the L-shaped spur dike with different wing lengths, so that with increasing the wing length of the L-shaped spur dike to the web, the maximum depth and volume of scouring has decreased. On the other hand, increasing the depth and volume of the scour has been directly related to increasing the position of placing the spur dike in the 90 degree bend. The results showed that with the entry of flow into the second half of the bend, the intensity of the depth and volume of scouring is significantly increased, so that the maximum depth and volume of scouring occurred at an angle of 90 degrees with a ratio of wing-to-web of 1. Subsequently, the lowest scouring depth occurred behind the spur dike in the 40 ° position with a wing-to-web ratio of 0.5.

It should be noted that in all cases, the horizontal velocity decreased with increasing wing length relative to the web of the spur dike. The results showed that the maximum flow velocity in the first half is inclined towards the outer bend and by entering the second half of the bend and colliding with the spur dike, it is inclined towards the inner bend.

The results showed that the SSIIM numerical model has a high ability and accuracy in simulating scour around the L-spur dike, so that the comparison between laboratory and numerical results shows a high correlation with the value of $R^2 = 0.91$.

References

1. Przedwojski B, Blazejewski R, Pilarczyk KW, (1995). River training techniques: Fundamentals, Techniques and Applications. AA. Balkema, Rotterdam, Netherlands. 1995. 686 pages.

2. Masjedi A, Foroushani E. Investigation of hydrodynamics on local scour by shape of single spur dike in river bend. 26th IAHR Symposium on Hydraulic Machinery and Systems, IOP Conference Series: Earth and Environmental Science 15(5), 2012.
3. Divsalar I, Musavi Jahromi, SH, (2014). Investigation of the Effect of Increasing the Wing Length of the L-Shape Spur Dike on the Scouring Around in the 90 Degree Bend. Journal of Irrigation Sciences and Engineering (JISE), 37(3): 53- 61.
4. Ahmad M. Experiments on design and behavior of spur-dikes. Proceedings of International Hydraulics Convention. Minneapolis, USA, 1953.
5. Garde RJ, Subramanya K, Nambudripad KD, (1961). Study of scour around spur dikes. Journal of the Hydraulics Division, ASCE, 87(HY6): 23-37.
6. Gill M A, (1972). Erosion of sand beds around spur dikes. Journal of the Hydraulics Division, ASCE, 98(HY9):1587-1602.
7. Melville BW, (1992). Local scour at bridge abutments. Journal of Hydraulic Engineering, ASCE, 118(4): 615-631.
8. Fazli M, Ghodsian M, Salehi SAA. Experimental investigation on scour around spur dikes located at different positions in a 90 bend. 32nd Congress of IAHR,Venice, Italy. 2007; pp: 248-256.
9. Zhang H, Nakagawa H, Kawaike K, Yasuyuki BA, (2009). Experiment and simulation of turbulent flow in local scour around a spur dyke. Int. J. Sediment Res, 24(1): 33-45.
10. Norouzi H, Salehi-Neishabori SA, Nasiri-Saleh F, Azarderakhsh M, (2009). Three-dimensional numerical simulation of scour around a spur dike. Modares Tech. Eng. J. 36, 13-22.
11. Yazdi J, Sarkardeh H, Azamathulla MDH, Aminuddin AB, (2010) .3D simulation of flow around a single spur dike with free-surface flow. International Journal of River Basin Management, 8(1): 55-62.
12. Abhari N M, Ghodsian M, Vaghefi M, Panahpura N, (2010). Experimental and numerical simulation of flow in a 90° bend. Flow Measurement and Instrumentation. 21(1): 292-298.
13. Ghobadian R, Mohammadi K, (2011). Simulation of subcritical flow pattern in 180° uniform and convergent open-channel bends using SSIIM 3-D model. Water Science and Engineering, 4(1): 270-283.
14. Vaghefi M, Ghodsian M, Salehi, S AA, (2012). Experimental study on scour around a T-Shaped spur dike in a channel bend. Journal of Hydraulic Engineering, 138(5): 471-474.
15. Karami H, Basser H, Ardeshir A, Hosseini HS, (2014). Verification of numerical study of scour around spur dikes using experimental data. Water and Environment Journal, 28(1),124–134.
16. Kiani A, Masjedi A, Pourmohammadi MH, Heidarnejad M, Bordbar A, (2017). Experiment of local scour around a series of spur dikes in river bend. Fresenius Environmental Bulletin, 26(8),5331-5339.
17. Vaghefi M, Ghodsian M, Akbari M, (2017). Experimental investigation on 3D flow around a single T-shaped spur dike in a bend. Period. Polytech. Civil Eng, 61(3): 462-470.
18. Oslen N R B. A. Three-Dimensional Numerical Model for Simulation of Sediment Movement in Water Intakes with Multi-Block Option. User's Manual. Department of Hydraulic and

Environmental Engineering, Norwegian University of Science and Technology, Norway, 2018.
19. Ning J, Li G, Li SH, (2019). Numerical Simulation of the Influence of Spur Dikes. Appl. Sci, 9(11), 2306.
20. Omenzadeh M R, Makvandi A, Aghamajidi R, (2019). Investigation of the effect of spur dike length on the scour depth near the spur dike at the 90-degree position and the 180-degree bend of the rivers. International Journal of Engineering and Technology, 11(1): 35-40.
21. Bahrami-Yarahmadi M, Pagliara S, Yabarehpour E, (2020). Study of Scour and Flow Patterns Around Triangular-Shaped Spur Dikes. KSCE Journal of Civil Engineering, 24(1): 3279–3288.
22. Rasaei M, Nazari S, Eslamian S, (2020). Experimental investigation of local scouring around the bridge piers located at a 90° convergent river bend. Sadhana, 45(1), 87.
23. Rasaei M, Nazari S, Eslamian S, (2020). Experimental and numerical investigation the effect of pier position on local scouring around bridge pier at a 90° convergent bend. Journal of hydraulic structures, 6(1): 55-76.
24. Rasaei.M, Nazari S, Eslamian S, (2020). Experimental and Numerical Investigation of Local Scouring around Bridge Piers in Different Geometric Shapes at a 90° Convergent meander. Journal of hydraulic structures, 6(2): 55-76.
25. Tripathi RP, Pandey KK, (2021). Experimental study of local scour around T-shaped spur dike in a meandering channel. Water Supply, 21(2): 542–552.
26. Olsen N R B. A three dimensional numerical model for simulation movement in water intakes with multiblock option. Department of hydraulic and Environmental Engineering, The Norwegian University of science and Technology, 2006.